



# The RyR2-R2474S Mutation Sensitizes Cardiomyocytes and Hearts to Catecholaminergic Stress-Induced Oxidation of the Mitochondrial Glutathione Pool

Jörg W. Wegener<sup>1,2,3</sup>, Ahmed Wagdi<sup>3,4</sup>, Eva Wagner<sup>1</sup>, Dörthe M. Katschinski<sup>3,4</sup>, Gerd Hasenfuss<sup>1,3</sup>, Tobias Brueggemann<sup>2,3,4</sup> and Stephan E. Lehnart<sup>1,2,3\*</sup>

<sup>1</sup> Department of Cardiology and Pulmonology, Heart Research Center Göttingen, University Medical Center Göttingen, Georg August University of Göttingen, Göttingen, Germany, <sup>2</sup> Cluster of Excellence "Multiscale Bioimaging: From Molecular Machines to Networks of Excitable Cells" (MBExC), Georg-August University of Göttingen, Göttingen, Germany, <sup>3</sup> DZHK (German Centre for Cardiovascular Research), Partner Site Göttingen, Göttingen, Germany, <sup>4</sup> Institute of Cardiovascular Physiology, University Medical Center Göttingen, Georg August University of Göttingen, Göttingen, Germany

## OPEN ACCESS

### Edited by:

Alexey V. Glukhov,  
University of Wisconsin-Madison,  
United States

### Reviewed by:

William E. Louch,  
University of Oslo, Norway  
Francisco J. Alvarado,  
University of Wisconsin-Madison,  
United States

### \*Correspondence:

Stephan E. Lehnart  
slehnart@med.uni-goettingen.edu

### Specialty section:

This article was submitted to  
Cardiac Electrophysiology,  
a section of the journal  
Frontiers in Physiology

**Received:** 15 September 2021

**Accepted:** 19 November 2021

**Published:** 09 December 2021

### Citation:

Wegener JW, Wagdi A, Wagner E, Katschinski DM, Hasenfuss G, Brueggemann T and Lehnart SE (2021) The RyR2-R2474S Mutation Sensitizes Cardiomyocytes and Hearts to Catecholaminergic Stress-Induced Oxidation of the Mitochondrial Glutathione Pool. *Front. Physiol.* 12:777770. doi: 10.3389/fphys.2021.777770

Missense mutations in the cardiac ryanodine receptor type 2 (RyR2) characteristically cause catecholaminergic arrhythmias. Reminiscent of the phenotype in patients, RyR2-R2474S knockin mice develop exercise-induced ventricular tachyarrhythmias. In cardiomyocytes, increased mitochondrial matrix  $\text{Ca}^{2+}$  uptake was recently linked to non-linearly enhanced ATP synthesis with important implications for cardiac redox metabolism. We hypothesize that catecholaminergic stimulation and contractile activity amplify mitochondrial oxidation pathologically in RyR2-R2474S cardiomyocytes. To investigate this question, we generated double transgenic RyR2-R2474S mice expressing a mitochondria-restricted fluorescent biosensor to monitor the glutathione redox potential ( $E_{\text{GSH}}$ ). Electrical field pacing-evoked RyR2-WT and RyR2-R2474S cardiomyocyte contractions resulted in a small but significant baseline  $E_{\text{GSH}}$  increase. Importantly,  $\beta$ -adrenergic stimulation resulted in excessive  $E_{\text{GSH}}$  oxidization of the mitochondrial matrix in RyR2-R2474S cardiomyocytes compared to baseline and RyR2-WT control. Physiologically  $\beta$ -adrenergic stimulation significantly increased mitochondrial  $E_{\text{GSH}}$  further in intact beating RyR2-R2474S but not in RyR2-WT control Langendorff perfused hearts. Finally, this catecholaminergic  $E_{\text{GSH}}$  increase was significantly attenuated following treatment with the RyR2 channel blocker dantrolene. Together, catecholaminergic stimulation and increased diastolic  $\text{Ca}^{2+}$  leak induce a strong, but dantrolene-inhibited mitochondrial  $E_{\text{GSH}}$  oxidization in RyR2-R2474S cardiomyocytes.

**Keywords:** ryanodine receptor, mitochondria, dantrolene, glutathione redox potential, RyR2  $\text{Ca}^{2+}$  leak, mitochondrial oxidation, reactive oxygen species (ROS)

**Abbreviations:** CPVT, catecholaminergic polymorphic ventricular tachycardia; Dan Dantrolene, dTG double transgenic; DTT, dithiothreitol; EFS, electrical field stimulation;  $E_{\text{GSH}}$ , glutathione redox potential; Iso, isoproterenol; roGFP, reduction-oxidation-sensitive green fluorescent protein; ROS, reactive oxygen species; RyR2, ryanodine receptor type 2; SR, sarcoplasmic reticulum; sTG, single transgenic.

## INTRODUCTION

In the heart, where ATP consumption is highest of any tissue,  $\text{Ca}^{2+}$  homeostasis in the mitochondrial matrix and ATP synthesis in the inner mitochondrial membrane are tightly controlled and interacting in a tissue (muscle)-specific manner regulated by the mitochondrial membrane potential (Wescott et al., 2019; Boyman et al., 2020; Boyman et al., 2021). Pathologically altered intracellular  $\text{Ca}^{2+}$  signaling and impaired bioenergetics due to mitochondrial dysfunction contribute to both ventricular tachyarrhythmia (VT) and heart failure development, at least in part through increased production of reactive oxygen species (ROS) (Zhou and Tian, 2018; Santulli et al., 2021). Under physiological conditions at rest, mitochondrial oxidative phosphorylation and ATP synthesis are accompanied by a low level of cardiac ROS generation mainly through byproducts of the electron transport chain (Murphy, 2009). However, increased stress and enhanced cardiac performance strongly augment mitochondrial respiratory activity significantly increasing ROS production (Bertero and Maack, 2018). Although several enzymatic systems protect cardiomyocyte function through ROS neutralization (Munzel et al., 2017), chronically compromised mitochondrial bioenergetics in heart disease may shift the balance toward increased oxidation of the glutathione (GSH) redox potential ( $E_{\text{GSH}}$ ) (Bertero and Maack, 2018), especially since an increased energy demand during sustained  $\beta$ -adrenergic stimulation was proposed to weaken mitochondrial antioxidant defense (Bovo et al., 2015). Notably, increased mitochondrial  $E_{\text{GSH}}$  oxidation itself is a quantitative live-cell indicator of a strongly increased ROS production, and hence may identify an early key disease process and mark the beginning of metabolic remodeling in the failing heart (Doenst et al., 2013).

Under physiological conditions of excitation-contraction (E-C) coupling,  $\text{Ca}^{2+}$  influx through voltage-gated L-type  $\text{Ca}^{2+}$  channels ( $\text{Ca}_v1.2$ ) activates mass intracellular  $\text{Ca}^{2+}$  release via ryanodine receptor type 2 (RyR2) large-conductance channels in the sarcoplasmic reticulum (SR). This  $\text{Ca}^{2+}$ -induced  $\text{Ca}^{2+}$  release increases the intracellular  $\text{Ca}^{2+}$  concentration throughout the myofilaments activating myocardial contraction (Bers, 2002), while it accounts for up to two-thirds of cardiac ATP consumption (Suga, 1990; Meyer et al., 1998). Vice versa, for cardiac relaxation intracellular  $\text{Ca}^{2+}$  is decreased mainly via the SR  $\text{Ca}^{2+}$ -ATPase (SERCA2a) and extruded by electrogenic trans-sarcolemmal  $\text{Na}^+/\text{Ca}^{2+}$  exchange (NCX). Hence, diastolic  $\text{Ca}^{2+}$  cycling accounts for an additional  $\sim 30\%$  of total energy consumption at baseline in healthy cardiomyocytes and in human heart tissue (Gibbs et al., 1988; Meyer et al., 1998).

Interestingly, pathophysiological changes in cytosolic  $\text{Ca}^{2+}$  cycling are widely accepted as a central cause of arrhythmias and contractile dysfunction in atrial and ventricular tissue (Bers, 2002; Alsina et al., 2019; Brandenburg et al., 2019; Dridi et al., 2020; Berisha et al., 2021; Boyman et al., 2021; Sadredini et al., 2021; Santulli et al., 2021). In this context, increased mitochondrial ROS generation can contribute to altered  $\text{Ca}^{2+}$  handling and vice versa, which may furthermore constitute a vicious cycle in cardiomyocytes (Zhou and Tian, 2018; Santulli et al., 2021).

However, the quantitative and molecular mechanisms if and how acutely increased SR  $\text{Ca}^{2+}$  leak causes excess mitochondrial  $\text{Ca}^{2+}$  uptake and ROS generation have been and continue to be controversially discussed (Mallilankaraman et al., 2012; Antony et al., 2016; Kohlhaas et al., 2017; Wescott et al., 2019; Boyman et al., 2020; Rossini and Filadi, 2020; Boyman et al., 2021; Santulli et al., 2021). Nonetheless, the largest known ion channel, RyR2, contains a relatively high number of redox-reactive cysteine residues and hence provides an important molecular substrate for increased ROS generation in cardiomyocytes (Santulli and Marks, 2015). For instance, RyR2 is oxidized in atrial tissue *in vivo* in a genetic model of catecholaminergic polymorphic ventricular tachycardia (CPVT), RyR2-R2474S<sup>+/-</sup> knockin mice, with increased susceptibility for pacing-induced atrial fibrillation (Shan et al., 2012).

Interestingly, while CPVT has been initially characterized solely as an arrhythmogenic cardiomyopathy (Yano et al., 2009), subsequently seizures originating in the brain (Lehnart et al., 2008; Lieve et al., 2019) and glucose intolerance in the Langerhans cells of the pancreas have been demonstrated in humans and mouse models (Santulli and Marks, 2015; Santulli et al., 2015). Although the majority of biophysically investigated RyR2 missense mutations point to a gain-of-function defect following protein kinase A phosphorylation both at the recombinant and native single-channel level (Wehrens et al., 2003; Lehnart et al., 2004; Tester et al., 2007; Lehnart et al., 2008), the role of PKA-dependent RyR2 phosphorylation remains controversial (Leenhardt et al., 2012; Wleklinski et al., 2020) since, e.g., inhibition of cardiac CaMKII by gene therapeutically applied CaMKII inhibitory peptide, but not PKA inhibitory peptide, effectively suppressed ventricular arrhythmias in a murine and an iPSC-CM model of CPVT (Bezzarides et al., 2019). However, a general consensus exists that adult cardiomyocytes and intact hearts from knockin mice expressing different gain-of-function RyR2 mutations are susceptible for significantly increased diastolic  $\text{Ca}^{2+}$  leak and  $\text{Ca}^{2+}$  waves following  $\beta$ -adrenergic stimulation (Lehnart et al., 2008; Fernandez-Velasco et al., 2009; Liu et al., 2009; Uchinoumi et al., 2010; Leenhardt et al., 2012; Borile et al., 2021). Strikingly, consistent with the human phenotype of a normal left-ventricular structure and function at rest, morphological and contractile changes have been excluded in a distinct independent RyR2-R2474S knockin mouse with a clear  $\beta$ -adrenergic driven phenotype of  $\text{Ca}^{2+}$  triggered cardiac VT (Uchinoumi et al., 2010). Given that the altered SR  $\text{Ca}^{2+}$  leak/load balance needs to be acutely compensated at the cost of increased ATP consumption during catecholaminergic stimulation (Eisner et al., 2020), CPVT-affected hearts may face a challenging metabolic state during episodes of transient intracellular  $\text{Ca}^{2+}$  overload and  $\beta$ -adrenergic stimulation, which may lead to increased mitochondrial  $\text{Ca}^{2+}$  load with excessive ROS generation and contribute to electrical and contractile cardiomyocyte dysfunction (Bers, 2014; Wescott et al., 2019; Boyman et al., 2021).

In the failing heart, ROS signaling has been established as a central process of the organic disease progression (Heymes et al., 2003; Yano et al., 2005; Guo et al., 2007; Akki et al., 2009). Increasing evidence suggests that excessive ROS

production can lead to chronic cardiac pathologies, such as apoptosis, fibrosis, and hypertrophy jointly promoting the maladaptive ventricular remodeling (von Harsdorf et al., 1999; Cucoranu et al., 2005; Takimoto et al., 2005; Hori and Nishida, 2009; Santulli et al., 2021). Recently, the mechanisms that temporally and spatially link excess ROS and  $\text{Ca}^{2+}$  as two principal detrimental factors have been addressed in the context of diabetic cardiomyopathy. Acute elevation of the extracellular glucose concentration induces cardiomyocyte ROS production through O-GlcNAcylation of CaMKII $\delta$  and activation of NOX2 (NADPH oxidase type 2) resulting in increased ROS production in the cytosol but not in the mitochondria (Lu et al., 2020). On the other hand, RyR2-R2474S $^{+/-}$  knockin mice exhibiting catecholamine-induced intracellular  $\text{Ca}^{2+}$  leak subsequently revealed mitochondrial dysfunction, increased ROS production, increased atrial RyR2 channel oxidation, and arrhythmia susceptibility (Xie et al., 2015). Moreover, inhibitory pharmacological treatment selectively targeting the RyR2  $\text{Ca}^{2+}$  leak or genetic inhibition of mitochondrial ROS production both prevented atrial fibrillation, indicating that RyR2 leakage and mitochondrial ROS generation may indeed constitute a self-enforcing subcellular cycle that can set off arrhythmias (Xie et al., 2015). However, the acute mechanism and hence direct but transient link of the catecholamine-stimulated RyR2-R2474S $^{+/-}$   $\text{Ca}^{2+}$  leak on mitochondrial ROS production have not been investigated previously.

Novel transgenic reporter mouse lines expressing the Grx1-roGFP GSH redox biosensor in a cardiomyocyte-restricted manner targeted to either the cytoplasm or the mitochondrial matrix have been established previously (Swain et al., 2016). Thus, cardiomyocytes from Grx1-roGFP biosensor mice allow the direct live-cell monitoring of changes in compartmentalized - cytosolic vs. mitochondrial -  $E_{\text{GSH}}$  (Swain et al., 2016), as demonstrated acutely in response to high extracellular glucose concentrations recently (Lu et al., 2020).

The objective of the present study is to investigate mitochondrial and cytosolic  $E_{\text{GSH}}$  changes during pacing-controlled contractions in RyR2-R2474S cardiomyocytes and intact hearts in a knockin mouse model of CPVT. To investigate the interplay between acute catecholamine-stimulated increased SR  $\text{Ca}^{2+}$  leak and mitochondrial oxidation changes, we crossed the mitochondrial matrix-targeted Grx1-roGFP (mito-Grx1-roGFP) redox biosensor line with mitochondrial redox-competent C57BL/6N background RyR2-R2474S $^{+/-}$  knockin mouse strain by heterozygous breeding (Lehnart et al., 2008; Nickel et al., 2015; Swain et al., 2016). While double transgenic mito-Grx1-roGFP:RyR2-R2474S $^{+/-}$  (RyR2-R2474S dTG) cardiomyocytes showed a significant  $E_{\text{GSH}}$  increase during pacing-evoked contractions following  $\beta$ -adrenergic stimulation compared to RyR2-WT control cardiomyocytes, *ex vivo* perfusion of isoproterenol-stimulated RyR2-R2474S dTG hearts significantly extended and confirmed the cellular findings. Importantly, acute treatment of RyR2-R2474S dTG-cardiomyocytes with the RyR channel blocker dantrolene diminished this  $E_{\text{GSH}}$  increase.

## MATERIALS AND METHODS

### Double-Transgenic and Single-Transgenic Mouse Lines

All animal procedures were reviewed by the institutional animal care and use committee of the University Medical Center Göttingen and the veterinarian state authority (protocol T11/2; LAVES, Oldenburg, Germany) in line with Directive 2010/63/EU of the European Parliament. Isolated cardiomyocytes and hearts were harvested either from heterozygous RyR2-R2474S dTG or RyR2-WT control mice expressing the mitochondria-restricted  $E_{\text{GSH}}$  biosensor in cardiomyocytes in the C57BL/6N background (Lehnart et al., 2008; Nickel et al., 2015; Swain et al., 2016). RyR2-WT control (mito-Grx1-roGFP2 $^{+/-}$ :RyR2 $^{+/+}$ ) and RyR2-R2474S dTG (mito-Grx1-roGFP2 $^{+/-}$ :RyR2 $^{\text{R2474S}/+}$ ) mice of either sex were humanely euthanized between 12 and 28 weeks age for heart extraction and/or ventricular cardiomyocyte isolation. In addition, cardiomyocytes isolated from single-transgenic (sTG) mouse hearts expressing the biosensor in the cytosol [cyto-Grx1-roGFP2 $^{+/-}$ ] were investigated following protocols reported previously (Swain et al., 2016)].

### Redox Biosensor Measurements and $E_{\text{GSH}}$ Calculation in Isolated Cardiomyocytes

Ventricular cardiomyocytes were isolated and quality controlled as described previously (Wagner et al., 2014; Peper et al., 2021). Isolated cardiomyocyte suspensions were plated onto laminin-coated glass coverslips (Imaging Dish CG 1.0, Zellkontakt, Nörten-Hardenberg, Germany) at room temperature. Only quiescent brick-shaped cardiomyocytes with cross-striations visualized at high contrast (e.g. see brightfield image below) were used if they contracted regularly in capture to electrical field stimulation (EFS; 4 ms,  $\pm$  20 V biphasic, 0.5 Hz, Myopacer, IonOptix, Westwood, MA, United States). Pacing-responsive cardiomyocytes then underwent repeated EFS-trains for 10, 30, and 60 s at 0.1, 1, or 3 Hz, respectively, for up to 20 min (see **Supplementary Figure 1**). Isolated cardiomyocytes developing sustained spontaneous contractile activity with a frequency above >0.1 Hz after EFS-pacing or during live-cell imaging were excluded from further analysis.

Cardiomyocyte redox biosensor measurements were performed on an inverted epifluorescence microscope (Axiovert Observer, Zeiss, Oberkochen, Germany) equipped with a 40x oil objective (Fluar 40x/1.3, Zeiss, Oberkochen, Germany). The roGFP2 biosensor was excited at 405 and 488 nm using a monochromator with 5 nm bandwidth (Polychrome V, Till Photonics, Gräfelfing, Germany). The emitted light was detected above >530 nm (filter set #49002, Chroma, Olching Germany) and recorded with a CMOS camera (PrimE, Photometrics, Birmingham, United Kingdom). Biosensor signal changes are represented as intensity ratio obtained at 405/488 nm excitation. Images were acquired at 1 Hz and single-cell ROIs were analyzed offline after background subtraction using proprietary software (Visiview version 3.1, Visitron Systems, Puchheim, Germany).

Cardiomyocytes with baseline intensity ratios below 0.15 were paced in series at 0.1, 1, or 3 Hz, respectively, for 10, 30, and 60 s while the redox biosensor signal changes were continuously monitored (for a schematic of the experimental protocol, please refer to **Supplementary Figure 1**). The non-paced interval between each pacing train lasted 2–3 min to establish steady-state conditions. Only after the baseline redox biosensor signal has reached a stable baseline steady-state, the subsequent EFS pacing period was executed.  $\text{H}_2\text{O}_2$  (200  $\mu\text{M}$ ) was applied at the end of each experiment to confirm the maximal exogenous increase in intensity ratio (positive control) to capture the maximally oxidized state of the redox biosensor. In some experiments, dithiothreitol (DTT, 1 mM) was applied additionally after  $\text{H}_2\text{O}_2$  treatment to obtain the maximal decrease of the redox roGFP2 biosensor signal for calculation of the glutathione redox potential ( $E_{\text{GSH}}$ ). Isoproterenol (100 nM) and dantrolene (5  $\mu\text{M}$ ) were applied acutely for 10 min or incubated for 120 min as indicated, respectively, before the start of the biosensor imaging experiment. All experiments were performed in the HEPES-buffered bath solution (composition in mM: NaCl 140, KCl 5.4,  $\text{MgCl}_2$  1.2,  $\text{CaCl}_2$  1.2,  $\text{Na}_2\text{HPO}_4$  0.3, HEPES 10, glucose 10; pH adjusted to 7.4 with NaOH).

$E_{\text{GSH}}$  (glutathione redox potential) calibration was performed by protocols reported previously (Gutscher et al., 2008; Swain et al., 2016).  $E_{\text{GSH}}$  values were calculated by analysis of the fluorescence intensities at 405 and 488 nm after treatment with  $\text{H}_2\text{O}_2$  (maximal oxidation) and DTT (maximal reduction). The redox potential  $E^0$  for roGFP2 was estimated to  $-280$  mV according to protocols published previously (Dooley et al., 2004).

## Whole Heart Imaging

Hearts from mito-Grx1-roGFP2<sup>+/-</sup>:RyR2<sup>+/+</sup> mice (WT control) and mito-Grx1-roGFP2<sup>+/-</sup>:RyR2<sup>R2474S/+</sup> mice (dTG) were quickly extracted after cervical dislocation and immediately placed in ice-cold Dulbecco's phosphate-buffered solution. Non-cardiac tissue was discarded, and the heart perfused via the aorta with Tyrode's solution (containing in mM: 1.8  $\text{CaCl}_2$ , 140 NaCl, 5.4 KCl, 2  $\text{MgCl}_2$ , 10 Glucose, 10 HEPES; pH adjusted to 7.4 using NaOH, bubbled with 100%  $\text{O}_2$  at 37°C). A bipolar epicardial electrogram was obtained using a silver electrode in contact with the right atrium and a metal spoon at the heart's apex. The signal was amplified (Animal Bio Amp FE136), recorded using PowerLab 16/35, and analyzed with LabChart 8.1.18 software, all ADInstruments, Oxford, United Kingdom. Hearts were placed in the optical path of a macroscope (MVX10, MVLPAPO1x, NA: 0.25, Olympus, Hamburg, Germany) connected through a light-guide ( $\varnothing$  2 mm, NA 0.5) with a LEDHub (Omicron-Laser, Rodgau, Germany). Hearts from WT control and dTG mice showed spontaneous beating rates of  $286 \pm 30$  ( $n = 4$ ) and  $217 \pm 32$  ( $n = 3$ ) bpm under untreated conditions, respectively, which increased to  $382 \pm 38$  ( $n = 4$ ) and  $322 \pm 50$  ( $n = 3$ ) bpm after  $\beta$ -adrenergic stimulation, respectively.

Hearts expressing the roGFP2 sensor were excited using the 385 nm LED and 460 nm LED within the LEDHub and the bandpass filters 385/26 and 475/23 nm (AHE, Tübingen, Germany), respectively. The light was sent to the epicardial surface and the emitted light was captured by the camera using

the filter set F46-002XL (AHE, Tübingen, Germany) without the excitation filter. Ratiometric images were acquired at a frame rate of 0.1 Hz using a custom-made software to synchronize both LEDs with the Zyla camera (Andor, Oxford Instruments, Oxford, United Kingdom) through NI 9263 CompactDAQ (National Instruments, Austin, TX, United States). Imaging and cardiac electrogram recording were performed during stable sinus rhythm and after isoproterenol stimulation (33 nM). At the end of each experiment,  $\text{H}_2\text{O}_2$  (200  $\mu\text{M}$ ) was applied followed by DTT (4 mM) to calibrate and calculate  $E_{\text{GSH}}$ .

## Confocal Imaging of Cardiomyocytes

Cardiomyocyte endomembrane structures were stained using the lipophilic fluorescent dye di-8-ANEPPS (50  $\mu\text{M}$ , Molecular Probes, Eugene, OR, United States) for 15 min at room temperature followed by two washing steps with buffer solution as reported previously (Wagner et al., 2014). Images were acquired with a confocal laser scanning microscope (LSM710, Carl Zeiss, Oberkochen, Germany) with a Plan-Apochromat  $\times 63/1.4$  oil Ph3 objective using 16x line averaging. For combined imaging of roGFP2 expressed in the mitochondrial matrix, the fluorescence excited at 490 nm was detected between 500 and 550 nm, and for di-8-ANEPPS, the fluorescence excited at 480 nm was detected between 550 and 650 nm. Pinhole was set to 0.8 AU.

## Chemicals

All chemicals were obtained from Sigma-Aldrich (Merck KGaA, Germany) unless otherwise indicated.

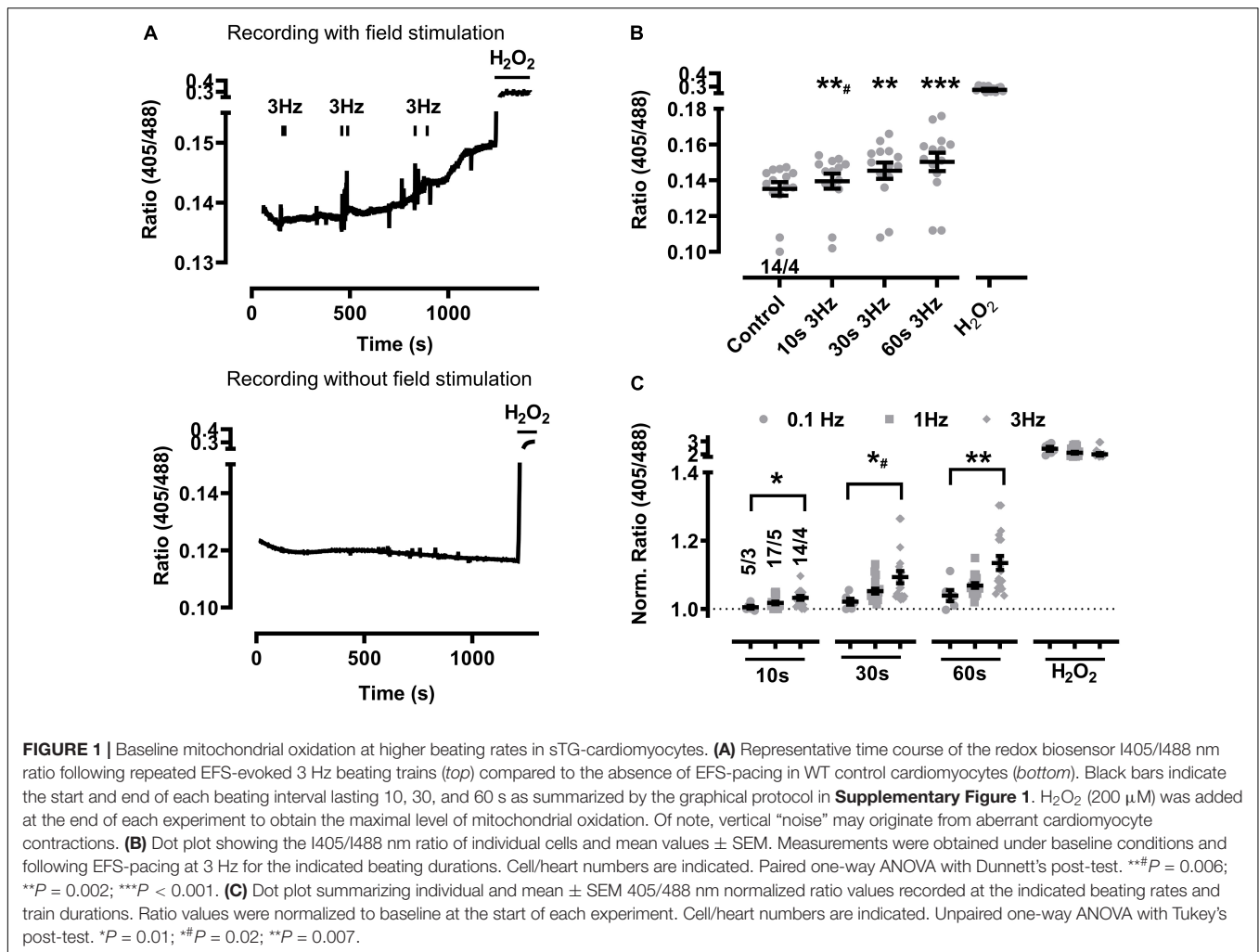
## Data Analysis

Data are reported as intensity ratio (I405/I488 in isolated cardiomyocytes and I385/I475 in whole hearts) or as ratio normalized to the baseline obtained at the start of each recording. Data analysis was performed with Prism 7 (GraphPad Software, San Diego, CA, United States). All data sets have passed a normality test (Kolmogorov-Smirnov). Statistical analysis between RyR2-WT control vs. RyR2-R2474S dTG cardiomyocytes was performed using paired or unpaired ANOVA with Dunnett's or Tukey's post-test as appropriate.

## RESULTS

### Baseline Mitochondrial Oxidation at Higher Beating Rates in sTG-Cardiomyocytes

Changes of the biosensor signal were initially characterized at increasing durations of pacing-evoked contractions in cardiomyocytes from sTG-mice expressing the redox reporter Grx1-roGFP2 targeted to either the mitochondrial matrix or the cytosol to confirm the imaging workflow as reported previously (Swain et al., 2016; Lu et al., 2020). Mito-Grx1-roGFP2 cardiomyocytes exhibited an apparent increase of the redox I405/I488 ratio after pacing when compared to non-paced



cells which was further increased by elongating the 3 Hz EFS-trains (**Figure 1A**). On average, 10 s of 3 Hz pacing with optically confirmed contractile pacing-capture was already sufficient to significantly increase mitochondrial oxidation (**Figure 1B**). Moreover, mitochondrial oxidation was further significantly increased by longer pacing durations both 30 and 60 s, while H<sub>2</sub>O<sub>2</sub> (200 μM) treatment confirmed the maximal level of the biosensor response (**Figure 1B**). Likewise, 10 s of 1 Hz pacing considerably increased mitochondrial oxidation which was further enhanced by longer pacing intervals of 30 and 60 s (**Figures 2A,B**). Of note, the original recording shows that the increase in the redox I405/I488 ratio after 30 s pacing at 1 Hz returned slowly to baseline over several minutes time indicating that the effect of pacing on the biosensor signal is reversible (**Figure 2A**). In summary, mitochondrial oxidation was significantly increased by pacing at 3 Hz compared to 0.1 Hz beating trains for 10, 30, and 60 s (**Figure 1C**).

In contrast, the cytosolic biosensor signals in cyto-Grx1-roGFP2 transgenic cardiomyocytes showed only non-significant smaller oxidation increases at 1 or 3 Hz beating, except when the 3 Hz beating rate lasted 60 s, while H<sub>2</sub>O<sub>2</sub> confirmed the maximal expected response (**Figure 3**). Taken together, these data

indicate that a stronger increase of the beating rate (e.g., from 0.1 to 1 and 3 Hz) leads to significantly increased oxidation of the mitochondrial GSH pool in a time-dependent manner (e.g., from 10 to 30 and 60 s), whereas a significant cytosolic oxidation increase was only observed after the longest (60 s long) 3 Hz beating rate.

## Preserved Transverse Tubule and Mitochondrial Network Interface in sTG-Cardiomyocytes

Accounting for ~30% of the cell volume of adult cardiomyocytes, it is anticipated that the regular subcellular inter-sarcomeric mitochondrial distribution is highly ordered between and along the myofilaments, as well as precisely juxtaposed by the junctional SR and transverse tubule (T-tubule) membrane invaginations at both mitochondria poles, where discontinuous T-tubule/SR contacts function as Ca<sup>2+</sup> release sites containing highly concentrated Ca<sub>v</sub>1.2 channels opposed to RyR2 clusters in nanometric proximity (recently reviewed in Rossini and Filadi, 2020). Whereas live-cell confocal mito-roGFP2 imaging showed the expected preserved inter-sarcomeric mitochondrial

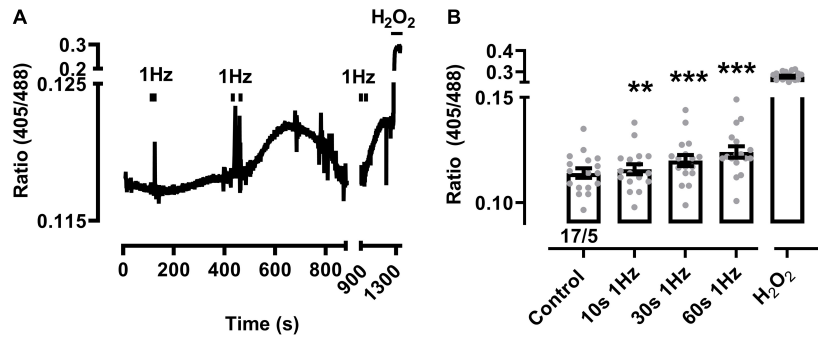


**FIGURE 2 |** Mitochondrial oxidation following prolonged 1 Hz beating in sTG-cardiomyocytes. **(A)** Representative time course of the redox biosensor I405/488 nm ratio with pacing-evoked 1 Hz beating trains in a mito-Grx1-roGFP2 cardiomyocyte. Black bars indicate the start and end of each beating interval lasting 10, 30, and 60 s, respectively. H<sub>2</sub>O<sub>2</sub> (200 μM) was added at the end of the experiment as indicated to confirm the maximal level of mitochondrial oxidation. The interval between 900 and 1,300 s was condensed to show the reversible signal changes after 30 s pacing. **(B)** Dot-bar plot showing the I405/488 nm ratio of the individual cardiomyocytes and mean values ± SEM. Measurements were obtained under baseline conditions and following EFS-pacing at 1 Hz for the indicated beating durations. Cell/heart numbers are indicated. Paired one-way ANOVA with Dunnett's post-test. \*\**P* = 0.007; \*\*\**P* < 0.001.

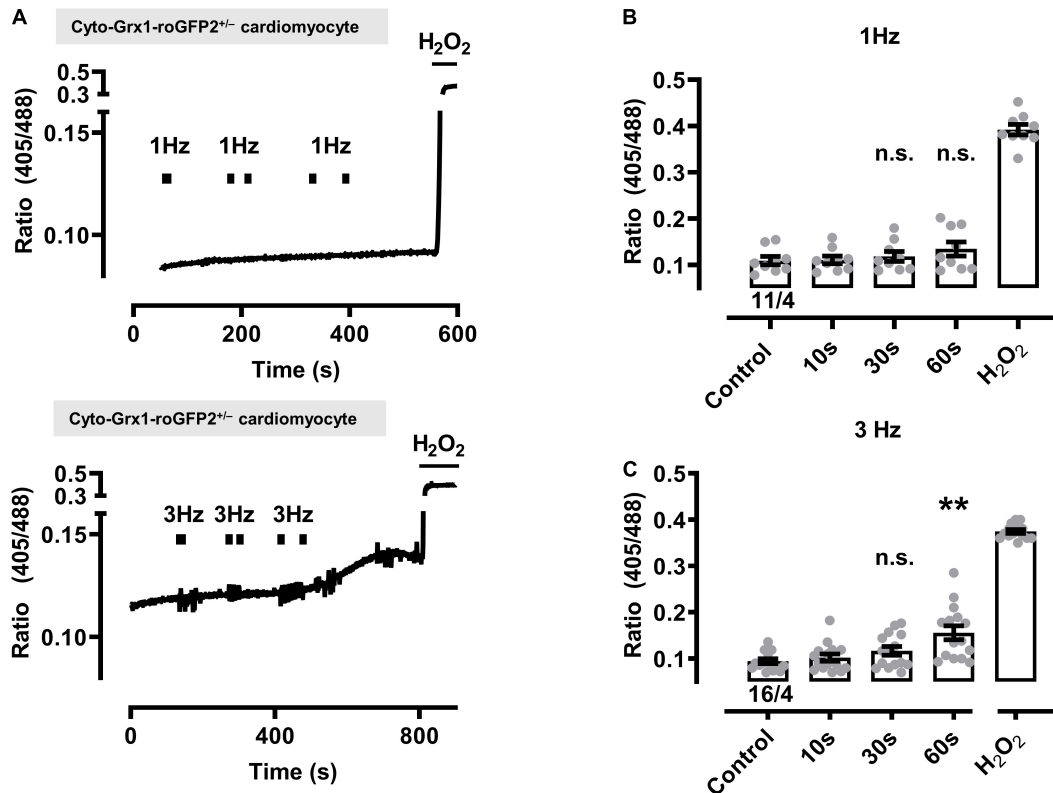


**FIGURE 3 |** Effect of contractile activity induced by electrical field stimulation (EFS) on the redox sensor signal in cardiomyocytes from cytosolic Grx1-roGFP2<sup>+/-</sup> mice. **(A)** Representative time course of the redox signal (ratio I405/488) with contractile activity by EFS at 1 Hz (above) and 3 Hz (below). Marks indicate the start and stop of the stimulation interval which lasted 10, 30, and 60 s, respectively. H<sub>2</sub>O<sub>2</sub> (200 μM) was added at the end of each experiment to obtain the maximal oxidized value. Up and down reflections of the signal represent low-frequency (<0.1 Hz) contractions of the myocyte. **(B)** Mean values ± SEM of ratio values obtained in cardiomyocytes under control conditions and after EFS at 1 Hz with a 10, 30, and 60 s duration. The signal values of each cardiomyocyte were obtained under control conditions and after the respective pacing. We used 11 cells from four mice as indicated. Statistical analysis was performed by paired one-way ANOVA with Dunnett's post-test. n.s., non-significant. **(C)** Mean values ± SEM of ratio values obtained in cardiomyocytes under control conditions and after EFS at 3 Hz with a 10, 30, and 60 s duration. We used 16 cells from four mice as indicated. Statistical analysis was performed by paired one-way ANOVA with Dunnett's post-test. \*\**P* = 0.008; n.s., non-significant.

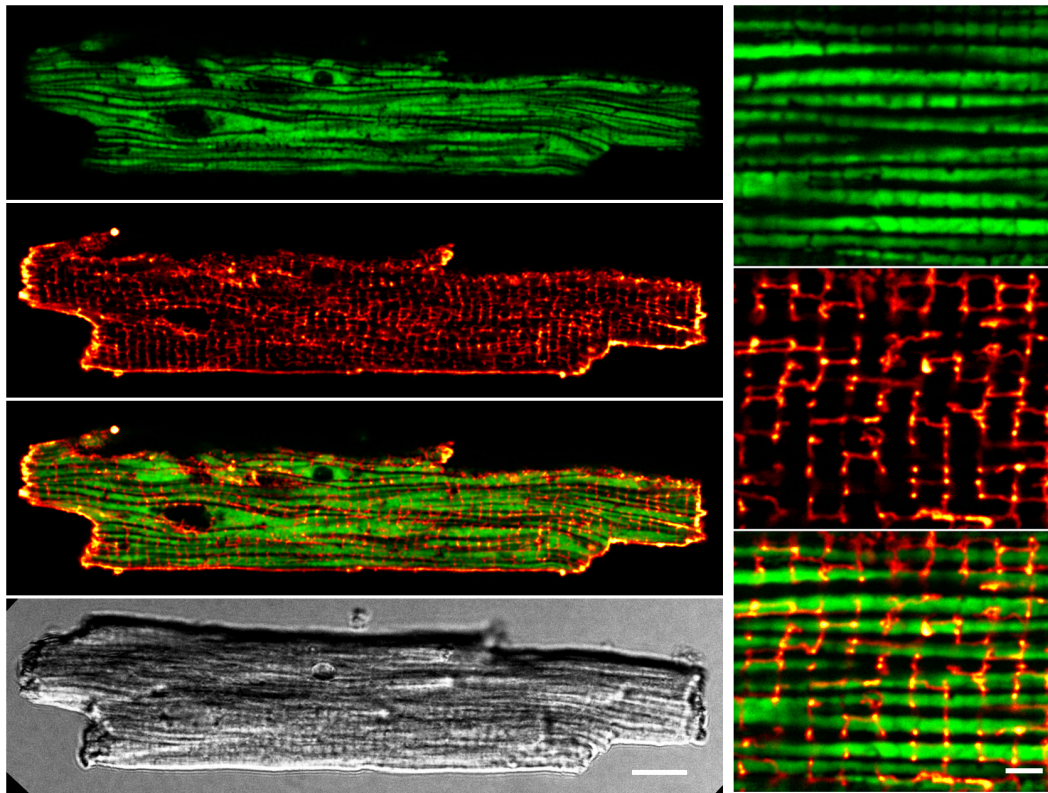


**FIGURE 4 |** Preserved transverse (T)-tubule and mitochondrial network interfaces in sTG-cardiomyocytes. Confocal live-cell images showing a representative ventricular cardiomyocyte expressing mitochondrial Grx1-roGFP2 after staining with the membrane dye di-8-ANEPPS. *Left* (from top to bottom): (i) roGFP2 auto-fluorescent signals (green LUT) demonstrating the longitudinal chain pattern typical for inter-sarcomeric mitochondria. (ii) di-8-ANEPPS membrane signal (red LUT) confirming a preserved, regular TAT membrane network mainly composed of T-tubule components. (iii) Overlay of the Grx1-roGFP2 and TAT membrane network signals showing a preserved gap-arrangement and confirming network interfaces of T-tubules and mitochondrial membranes. (iv) Cell quality and membrane integrity was confirmed by transmission scanning microscopy with differential interference contrast detecting regular transverse striations and sharp brick-shaped cell edges. Scale bar 10  $\mu\text{m}$ . *Right* (from top to bottom): zoom-in magnifications (i–iii) visualize the distinct mitochondrial and T-tubule compartments and interfaces. Scale bar 2  $\mu\text{m}$ .

density apparent as mature longitudinal chain architecture, the transverse-axial-tubule network furthermore revealed the expected invagination network components mainly composed of T-tubules (**Figure 4**) as reported previously in living mouse cardiomyocytes (Wagner et al., 2012). Apparently, the high T-tubule density regularly intersects the longitudinal mitochondrial strands perpendicularly in register (**Figure 4 overlay magnification**). These live-cell data indicate that the transgenic mito-roGFP2 expression did not affect the mechano-sensitive electrical conduction conduits in cardiomyocytes, which is an important prerequisite for a preserved excitation-bioenergetic coupling of the mitochondrial matrix reported recently (Wescott et al., 2019; Boyman et al., 2020; Boyman et al., 2021).

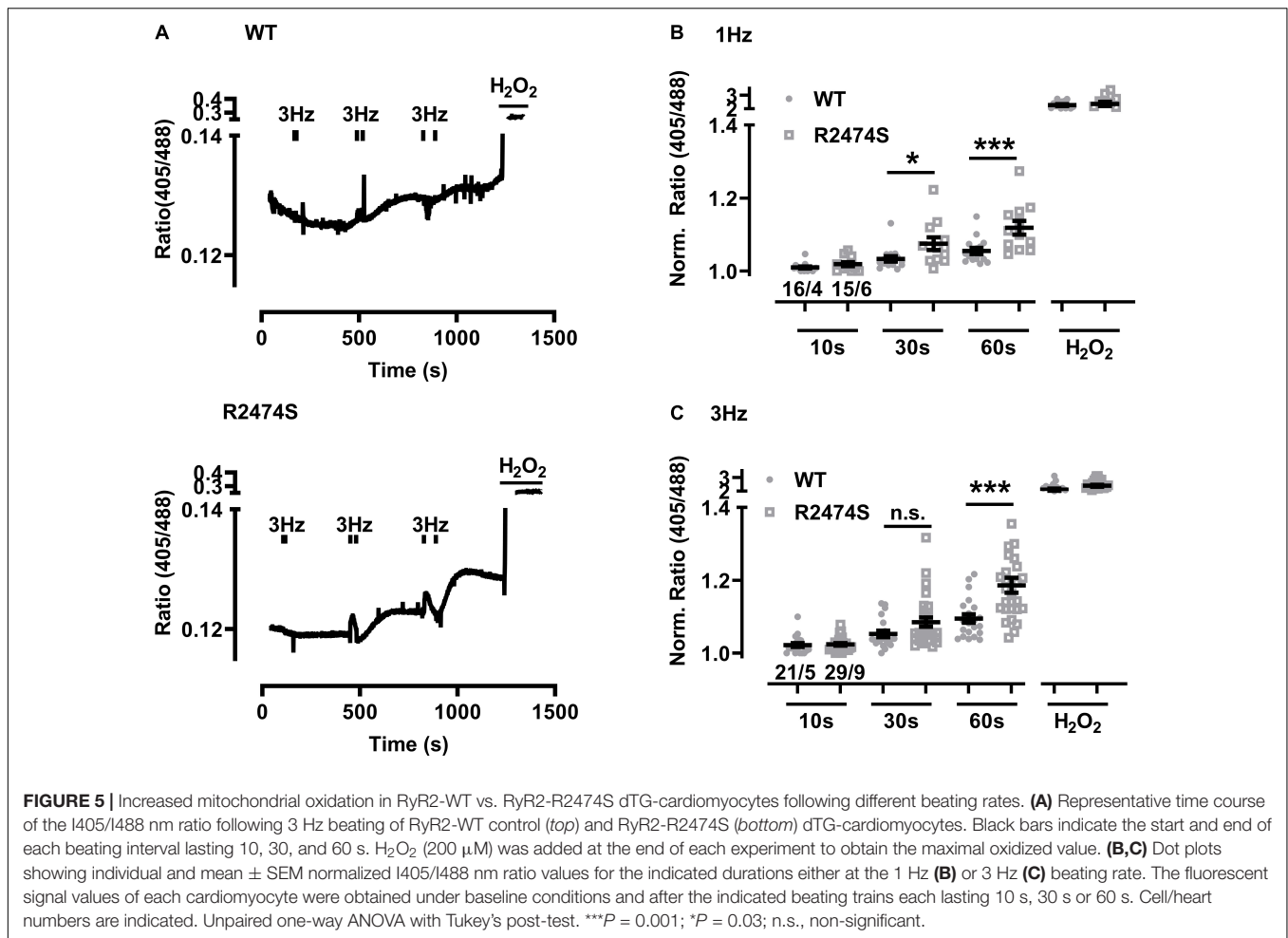
### Increased Mitochondrial Oxidation in RyR2-R2474S dTG-Cardiomyocytes

Next we extended the post-pacing mitochondrial  $E_{GSH}$  imaging to dTG-cardiomyocytes from mouse hearts additionally expressing the heterozygous RyR2-R2474S mutated tetrameric

$\text{Ca}^{2+}$  release channels vs. RyR2-WT control cells. Apparently, relatively large changes in mitochondrial oxidation were readily evidenced in RyR2-R2474S dTG-cardiomyocytes compared to RyR2-WT control (**Figure 5A**) particularly following 30 and 60 s of 1 Hz (**Figure 5B**) and 3 Hz pacing-evoked beating (**Figure 5C**). Together these data suggest that mitochondrial oxidation is significantly increased in heterozygous RyR2-R2474S dTG-cardiomyocytes by the identical 1 and 3 Hz beating rate pacing-trains compared to RyR2-WT control cells.

### $\beta$ -Adrenergic Stimulation Exacerbates Mitochondrial Oxidation in RyR2-R2474S dTG-Cardiomyocytes

An increased sympathetic tone, exercise, and an increased heart rate provoke the characteristic cardiac CPVT phenotype leading to VT episodes in humans (Lehnart et al., 2004; Danielsen et al., 2018; Baltogiannis et al., 2019). Consequently, isolated cardiomyocytes were exposed to selective  $\beta$ -adrenergic stimulation (isoproterenol 100 nM) and pacing (**Figure 6A**). First, mitochondrial oxidation was significantly increased



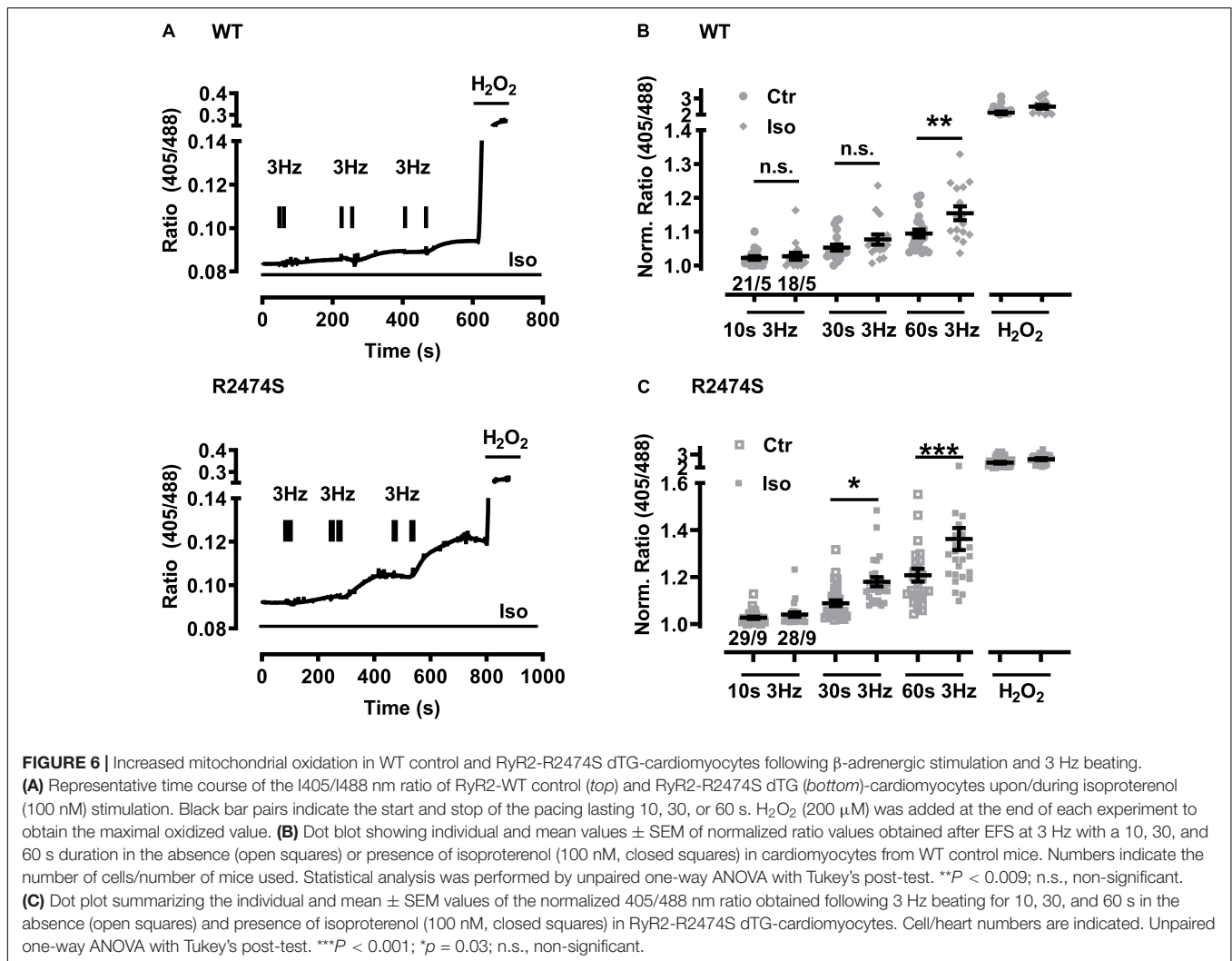
by isoproterenol-stimulation in WT control (**Figure 6B**) and RyR2-R2474S dTG-cardiomyocytes (**Figure 6C**) when compared to the untreated control cardiomyocytes, respectively. Notably, the isoproterenol-stimulation robustly increased mitochondrial oxidation already at post-30 s beating at 3 Hz in RyR2-R2474S dTG-cardiomyocytes compared to control (**Figure 6C**). Second, isoproterenol-treatment increased mitochondrial oxidation to a significantly larger extent in RyR2-R2474S dTG-cardiomyocytes compared to RyR2-WT control cells at the 3 Hz beating rate both after 30 and 60 s (**Figure 7A**) and even already at the lower 1 Hz beating rate after 60 s (**Figure 7B**). Third, mathematical quantification of the  $E_{GSH}$  revealed a significant depolarization/oxidation of over 10 mV following isoproterenol-treatment in RyR2-R2474S dTG-cardiomyocytes and a similarly increased oxidation at baseline and isoproterenol-stimulated between RyR2-R2474S dTG-cardiomyocytes and RyR2-WT control cells (**Figure 8**). Baseline  $E_{GSH}$  was not different between RyR2-WT control and RyR2-R2474S dTG-cardiomyocytes. Mean calculated  $E_{GSH}$  values ± SEM (in mV) were  $-290.9 \pm 2.2$  ( $n = 8$ ) and  $-288.8 \pm 3.4$  ( $n = 9$ ), respectively. As the level of mitochondrial oxidation was overall robustly increased after isoproterenol-stimulation when compared to non-treated

control RyR2-R2474S dTG-cardiomyocytes (**Figure 7**), β-adrenergic stimulation clearly exacerbated the mitochondrial glutathione oxidation.

### Isoproterenol Strongly Increases Mitochondrial Oxidation in Intact RyR2-R2474S dTG-Hearts

To monitor mitochondrial oxidation in the intact beating heart, RyR2-WT control and RyR2-R2474S dTG-hearts were Langendorff-perfused and the ventricular left and right epicardial surface imaged with simultaneous surface field-electrogram rhythm recordings. While color-coded mapping of the RyR2-WT dTG-heart apparently captured no major ventricular mitochondrial  $E_{GSH}$  change following acute β-adrenergic stimulation by isoproterenol (33 nM) in RyR2-WT control hearts (**Figure 9B**), a robust mitochondrial oxidation increase was evident in the beating RyR2-R2474S dTG-heart (**Figure 9A**). Meanwhile, both genetic heart groups showed the expected maximally increased oxidation by H<sub>2</sub>O<sub>2</sub> vs. a maximally decreased oxidation after adding DTT (**Figures 9A–C**).

Comparing the isoproterenol-stimulated  $E_{GSH}$  changes confirmed a significant mitochondrial oxidation increase in



RyR2-R2474S dTG-hearts, which was, however, not observed in RyR2-WT ventricles (Figure 9D). Together, these results significantly extend and further confirm the findings mainly documented in isolated RyR2-R2474S dTG-cardiomyocytes, underlining a significantly more oxidized mitochondrial state in beating dTG-hearts following  $\beta$ -adrenergic stimulation evidenced by the pronounced changes of the redox signal I385/I475 ratio monitoring acute  $E_{GSH}$  tissue changes.

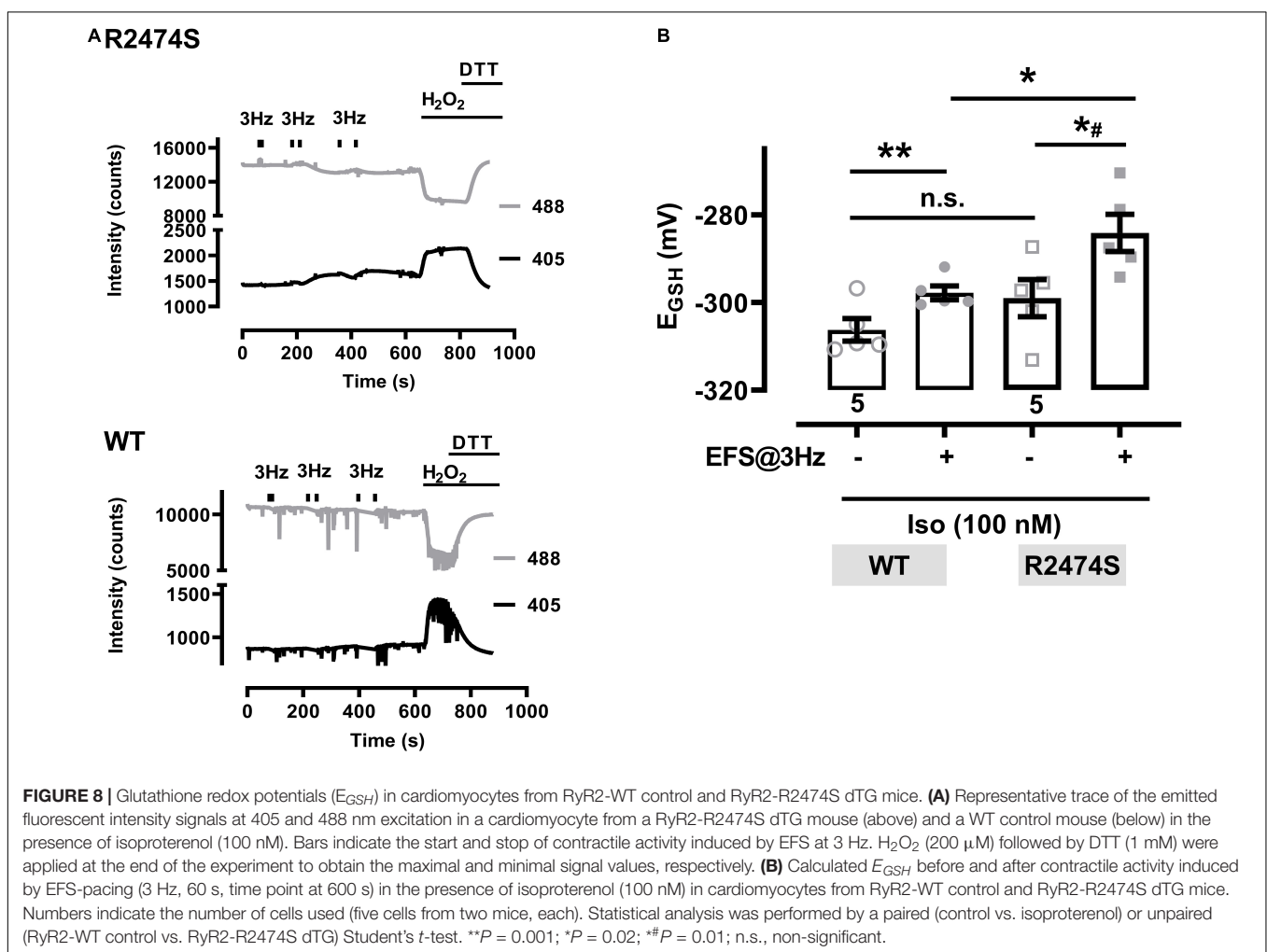
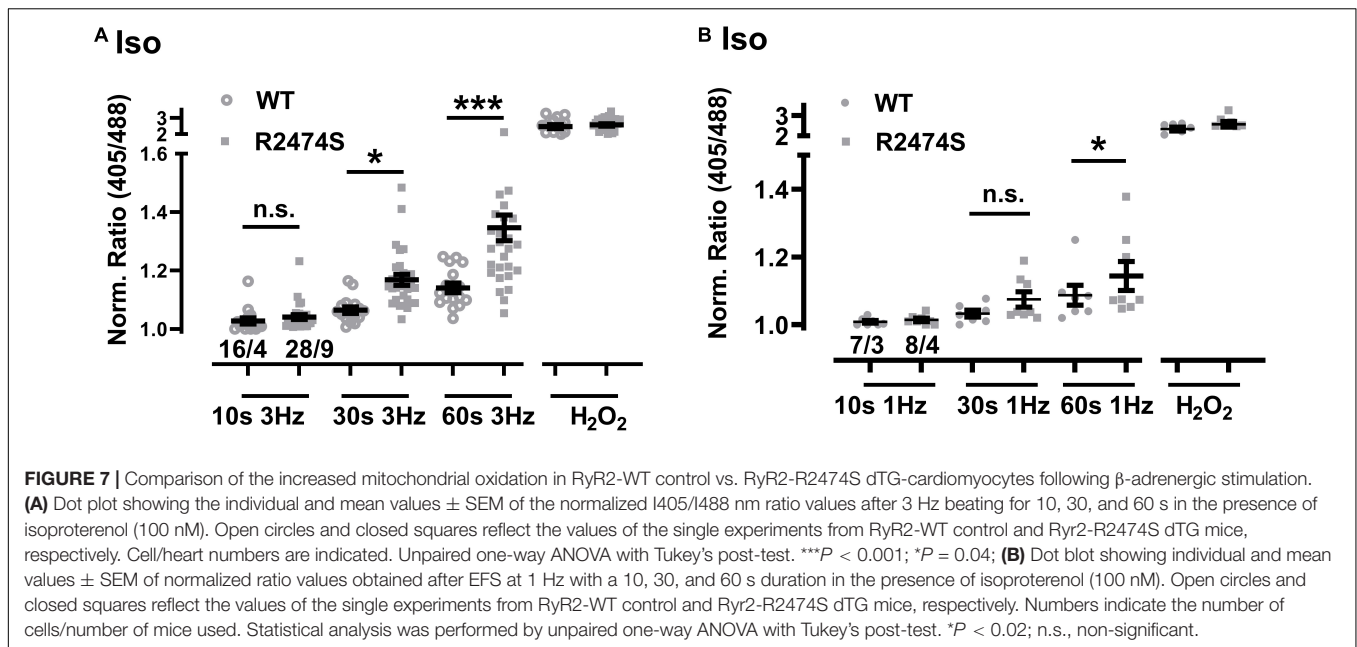
### Dantrolene Prevents Mitochondrial Oxidation in RyR2-R2474S dTG-Cardiomyocytes

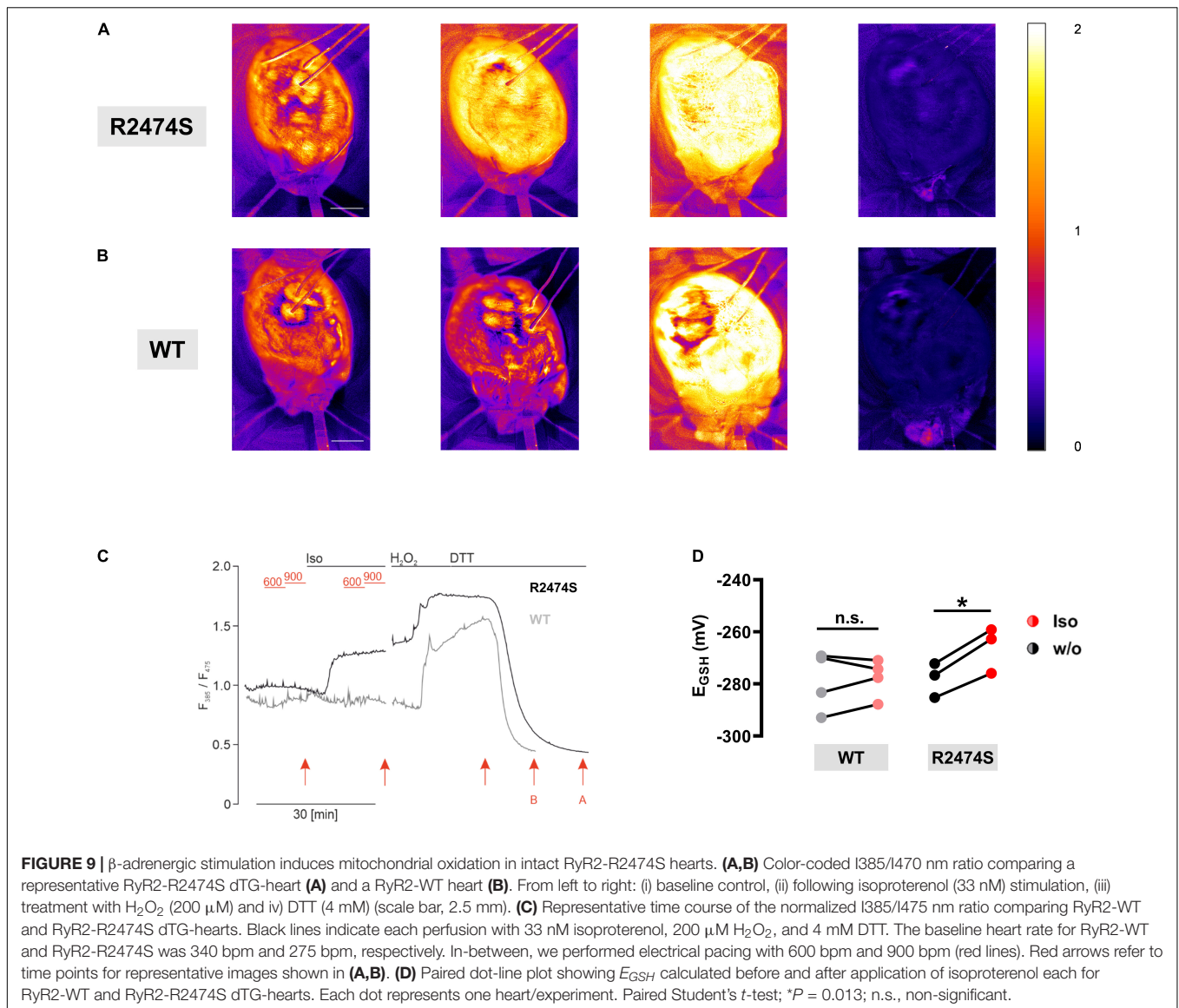
Dantrolene is used clinically as acute RyR1 channel blocker targeted to skeletal muscles and other tissues as emergency intervention to treat patients who develop life-threatening malignant hyperthermia episodes induced by certain anesthetic drug compounds during surgical interventions. Recent studies demonstrated that dantrolene may also cause beneficial antagonistic effects against the chronic cardiac RyR2 channel  $Ca^{2+}$  leak in human diseased cardiomyocytes isolated

from failing hearts (Hartmann et al., 2017). Therefore, the acute potential of the large-conductance channel-inhibitory efficacy of dantrolene against mitochondrial oxidation was investigated in RyR2-R2474S dTG-cardiomyocytes following  $\beta$ -adrenergic stimulation (isoproterenol 100 nM). Strikingly, dantrolene pre-treatment (5  $\mu$ M for 2 h) significantly decreased the large mitochondrial oxidation after 3 Hz 60 s-beating and non-significantly after 3 Hz 30 s-pacing (Figure 10). In summary, these data suggest that a pathologically increased mitochondrial oxidation in isoproterenol-stimulated RyR2-R2474S cardiomyocytes can be partly prevented by pharmacological dantrolene treatment.

## DISCUSSION

This work has examined how mitochondrial  $E_{GSH}$  oxidation is increased by essential factors in cardiomyocytes with important physiological and pathophysiological consequences that converge at the dynamic interface between RyR2 channel function, sympathetic catecholaminergic stimulation, and contractile



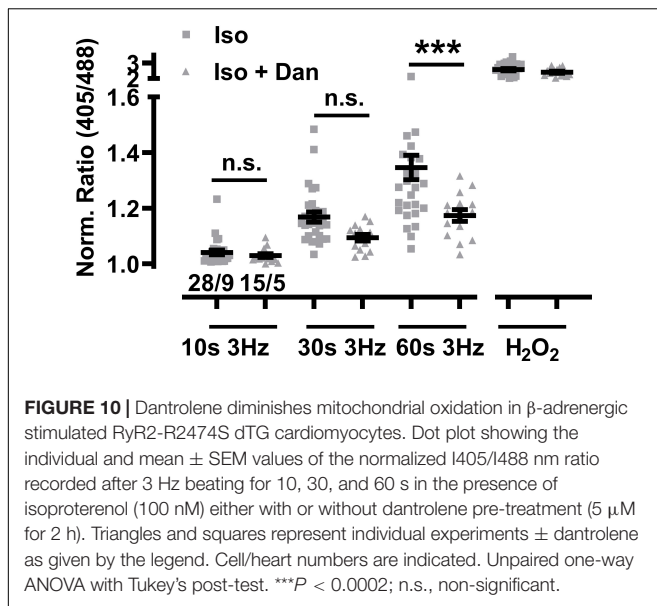


activity. Overall, we find that a significant increase following  $\beta$ -adrenergic stimulation significantly changes mitochondrial  $E_{\text{GSH}}$  in dTG-cardiomyocytes and hearts, which was further dependent on both the presence of the RyR2-R2474S missense mutation and faster beating rates. Importantly, dantrolene treatment of RyR2-R2474S dTG-cardiomyocytes results in a pronounced reduction of this increased mitochondrial oxidation. We discuss our findings on these interrelated RyR2-R2474S regulatory and  $E_{\text{GSH}}$  driven mitochondrial mechanisms in the context of previously published reports.

Recent quantitative imaging studies established that an increase of mitochondrial  $\text{Ca}^{2+}$  uptake was necessary to drive inner mitochondrial membrane depolarization and enhanced ATP synthesis in a heart-specific and previously unknown voltage-dependent fashion (Wescott et al., 2019; Boyman et al., 2020; Boyman et al., 2021). This contrasts with heart disease where alterations of mitochondrial  $E_{\text{GSH}}$  may profoundly

shift organelle metabolism and thus cardiac bioenergetics (Bertero and Maack, 2018). Beyond bioenergetics, increased mitochondrial  $E_{\text{GSH}}$  oxidation revealed a strongly increased ROS production, which might be of immediate relevance for heart disease progression and metabolic remodeling (Doenst et al., 2013). In analogy, increased mitochondrial oxidation and  $E_{\text{GSH}}$  depolarization in RyR2-R2474S cardiomyocytes and hearts indicate a strongly boosted ROS generation during faster beating rates concurrent with  $\beta$ -adrenergic stimulation.

Interestingly, increased SR  $\text{Ca}^{2+}$  leak and mitochondrial dysfunction have been demonstrated to enhance ROS production in heart disease previously (Zhou and Tian, 2018; Santulli et al., 2021). Remarkably, mitochondrial ROS scavenging attenuated the effects of augmented RyR2 activity leading to proarrhythmic  $\text{Ca}^{2+}$  waves in Calsequestrin2-null mice serving as a model for CPVT (Hamilton et al., 2020). In line with this view, ROS scavenging by mito-TEMPO was shown



to reduce the number of  $\text{Ca}^{2+}$  waves also in cardiomyocytes from rabbit hearts (Bovo et al., 2012; Cooper et al., 2013). As isoproterenol-stimulated RyR2-R2474S cardiomyocytes exhibit an over threefold increased  $\text{Ca}^{2+}$  spark frequency that additionally sustains regenerative intracellular  $\text{Ca}^{2+}$  waves, here the observed robust increase in mitochondrial oxidation will depend both on acute catecholamine stimulation and the beating rate-dependent extent and complex spatiotemporal dynamics of the cell-wide diastolic  $\text{Ca}^{2+}$  leak reported previously (Lehnart et al., 2008; Xie et al., 2015; Sadredini et al., 2021). However, even under physiological conditions, an increased mitochondrial oxidation was evidenced at higher beating rates in sTG-cardiomyocytes albeit much more pronounced in RyR2-R2474S dTG-cardiomyocytes. For the latter, the faster beating rate clearly led to mitochondrial  $E_{\text{GSH}}$  oxidation and this was most strongly increased after  $\beta$ -adrenergic stimulation.

Tight control of nanomolar diastolic  $\text{Ca}^{2+}$  levels is essential for normal cardiac function depending on the precise balance between cytosolic  $\text{Ca}^{2+}$  influx and efflux (Eisner et al., 2020). If the local control mechanisms become compromised, cardiomyocytes will develop arrhythmia and hypercontraction from cytosolic  $\text{Ca}^{2+}$  overload. This balance is disturbed when the diastolic  $\text{Ca}^{2+}$  spark frequency is significantly increased, a phenomenon linked molecularly to RyR2 channel gain-of-function defects (Cheng and Lederer, 2008; Bers, 2014). Interestingly, more than a dozen RyR2 mutations originally identified in CPVT patients have been shown to increase  $\text{Ca}^{2+}$  leak (Jiang et al., 2002; Wehrens et al., 2003; Lehnart et al., 2004; Kontula et al., 2005; Tester et al., 2007; Lehnart et al., 2008; Marjamaa et al., 2011; Shan et al., 2012). However, only two knockin models were confirmed to exhibit exercise-triggered VTs, RyR2-R2474S $^{+/-}$  (Lehnart et al., 2008) and RyR2-R4496C $^{+/-}$  (Priori and Napolitano, 2005; Liu et al., 2006), and are hence reminiscent of the human arrhythmia

phenotype diagnosed by exercise stress testing. In line with the *in vivo* pathology, RyR2-R2474S $^{+/-}$  cardiomyocytes exhibited an overall normal diastolic  $\text{Ca}^{2+}$  spark behavior at rest, but a strong spark frequency increase occurred after isoproterenol treatment (Lehnart et al., 2008). In this context, increased diastolic  $\text{Ca}^{2+}$  extrusion mainly by SERCA2a and NCX will necessarily consume additional ATP at rest at the cost of concomitantly increased ROS generation (Bers, 2002, 2014). Thus, our data further link increased catecholaminergic RyR2 channel dysfunction in a murine CPVT model to acute mitochondrial oxidation.

In the present study, we monitored the effect of increased contractile activity on  $E_{\text{GSH}}$  in the mitochondrial matrix, while the former process has been long known to correlate with mitochondrial metabolic activity and ROS generation (Gudbjarnason et al., 1962). Since a similar extent of  $E_{\text{GSH}}$  change was excluded in the cytoplasm, NOX2 seems unlikely as ROS source here (Santos et al., 2011). In another context, high extracellular glucose concentrations increased  $E_{\text{GSH}}$  in the cytosol through NOX2 but not in the mitochondrial matrix (Lu et al., 2020). In contrast, we found that mitochondrial oxidation depended on the duration and frequency of dTG-cardiomyocyte beating. This finding is in line with reported changes of NADH in response to a stepwise increase of the beating frequency from 0.1 to 3.3 Hz in guinea-pig cardiomyocytes (Jo et al., 2006). As the increase in the mitochondrial  $E_{\text{GSH}}$  following beating was observed both in RyR2-WT and RyR2-R2474S dTG-cardiomyocytes, a relation with increased SR  $\text{Ca}^{2+}$  leak seems plausible after pacing-evoked contractile activity reported previously (Sato et al., 1997). Finally, blocking RyR2  $\text{Ca}^{2+}$  leak with dantrolene diminished  $E_{\text{GSH}}$  oxidation as hypothesized previously (Hartmann et al., 2017).

A recent study demonstrated that  $\text{Ca}^{2+}$  leak increased mitochondrial ROS production in cultured WT rat cardiomyocytes transfected for 48 h with the OMM-HyPer mito-ROS biosensor (Hamilton et al., 2020). An increased ROS production has also been demonstrated during increased beating in healthy cardiomyocytes with the fluorescent probe dichlorodihydrofluorescein, which is confirmed by our sTG-cardiomyocyte data (Heinzel et al., 2006). In rat trabeculae, NADH oxidation was observed at 0.25–2 Hz after 60 s with pronounced ATP hydrolysis (Brandes and Bers, 2002). A similar time frame in response to contractile activity was observed in the present study, where the maximal change of the biosensor signal occurred within 2–3 min after beating. This further agrees with the reported change of the redox signal observed in cardiomyocytes in the same biosensor cardiomyocytes after a high glucose or pH challenge (Lu et al., 2020; Kreitmeyer et al., 2021). Since the observed redox changes occurred only after completion of the given beating period, it is suggested to correlate further with the aftercontraction related metabolic activity observed frequently in isoproterenol-stimulated RyR2-R2474S dTG-cardiomyocytes.

Importantly, our report provides the first evidence that  $E_{\text{GSH}}$  changes happen under quasi physiological conditions in the intact beating heart as well. Using the genetically encoded reporter targeted to mitochondria allowed to monitor the average  $E_{\text{GSH}}$  from the whole ventricular, anterior heart surface

(**Supplementary Videos 1, 2**) and to perform a ratiometric imaging excluding any major interference due to cardiac contractions. In comparison to the first description of the glutathione redox sensor mouse lines, we were able to increase the ratio differences from maximal oxidization to reduction to comparable signal-to-noise values to single-cell measurements (see **Figures 5, 9**). This increase in signal amplitude was the key for the detection of the comparable relatively small steps in oxidization during  $\beta$ -adrenergic stimulation, which we could only detect in the intact hearts of dTG mice expressing the RyR2-R2474S mutated channels. However, in contrast to isolated cardiomyocytes, we could not detect a change in oxidation by additional faster pacing in the spontaneously beating Langendorff hearts. One possible explanation may be that these changes are in comparison subtle and thus still not detectable in this setting. The other is that we focused on the effects of isoproterenol and such changes would occur only after prolonged phases of pacing which we could not implement in these experiments.

In summary, we have shown that contractile activity induced by EFS-pacing in isolated cardiomyocytes increased the mitochondrial  $E_{GSH}$  to more oxidized levels in a time- and frequency-dependent manner. The increase was most pronounced after  $\beta$ -adrenergic stimulation and in cardiomyocytes expressing the human RyR2-R2474S mutated tetrameric channel. The catecholaminergic  $E_{GSH}$  increase, however, was significantly attenuated by the pharmacological RyR2 channel antagonist dantrolene. Likewise, we observe a larger increase in the mitochondrial  $E_{GSH}$  toward more oxidized levels in spontaneously beating hearts expressing the RyR2-R2474S mutated channels after  $\beta$ -adrenergic stimulation as compared to control hearts. Hence, we suggest that the RyR2-R2474S mutation induces a metabolic burden in cardiomyocytes through excess ROS generation, especially after  $\beta$ -adrenergic stimulation, tipping the balance from a compensated to a high energetic cost and acutely increased diastolic  $Ca^{2+}$  leak, a multifactorial process, which may acutely contribute to the development of the arrhythmogenic CPVT phenotype as proposed for calsequestrin2-null mice previously (Hamilton et al., 2020).

## DATA AVAILABILITY STATEMENT

The original contributions presented in the study are included in the article/**Supplementary Material**, further inquiries can be directed to the corresponding author/s.

## REFERENCES

- Akki, A., Zhang, M., Murdoch, C., Brewer, A., and Shah, A. M. (2009). NADPH oxidase signaling and cardiac myocyte function. *J. Mol. Cell Cardiol.* 47, 15–22. doi: 10.1016/j.yjmcc.2009.04.004
- Alsina, K. M., Hulsurkar, M., Brandenburg, S., Kownatzki-Danger, D., Lenz, C., Urlaub, H., et al. (2019). Loss of protein phosphatase 1 regulatory subunit PPP1R3A promotes atrial fibrillation. *Circulation* 140, 681–693. doi: 10.1161/CIRCULATIONAHA.119.039642
- Antony, A. N., Paillard, M., Moffat, C., Juskeviciute, E., Correnti, J., Bolon, B., et al. (2016). MICU1 regulation of mitochondrial  $Ca(2+)$  uptake dictates

## ETHICS STATEMENT

The animal study was reviewed and approved by the Institutional IACUC. This study has not used *in vivo* examination of mice but *ex vivo* investigations, which are not subject to an ethics protocol at our institution.

## AUTHOR CONTRIBUTIONS

JW and AW performed the research and analyzed the data. JW, TB, DK, and SL wrote the manuscript. DK contributed to the biosensor mouse models and analyzed the data. JW, SL, TB, and GH designed the study. All authors approved the manuscript.

## FUNDING

This work was supported by grants from Deutsche Forschungsgemeinschaft SFB1002 to SL (projects A09 and S02), TB (A14), and GH (project D01), Germany's Excellence Strategy (EXC 2067/1-390729940) to SL, and SPP1926 to TB and SL. JW and AW were supported by DZHK (German Centre for Cardiovascular Research) Partner Site GÄttingen. SL is a principal investigator of DZHK.

## ACKNOWLEDGMENTS

Excellent technical assistance by Birgit Schumann is gratefully acknowledged.

## SUPPLEMENTARY MATERIAL

The Supplementary Material for this article can be found online at: <https://www.frontiersin.org/articles/10.3389/fphys.2021.777770/full#supplementary-material>

**Supplementary Video 1** | Color coded I385/I475 nm ratio comparing representative RyR2-WT hearts. Showing the ratio images during baseline control, isoproterenol (33 nM) stimulation, treatment with  $H_2O_2$  (200  $\mu$ M), and DTT (4 mM). Scale bar = 5 mm.

**Supplementary Video 2** | Color coded I385/I475 nm ratio comparing representative RyR2-R2474S dTG-hearts. Showing the ratio images during baseline control, isoproterenol (33 nM) stimulation, treatment with  $H_2O_2$  (200  $\mu$ M), and DTT (4 mM). Scale bar = 5 mm.

- survival and tissue regeneration. *Nat. Commun.* 7:10955. doi: 10.1038/ncomms10955
- Baltogiannis, G. G., Lysitsas, D. N., Di Giovanni, G., Ciconte, G., Sieira, J., Conte, G., et al. (2019). CPVT: arrhythmogenesis, therapeutic management, and future perspectives. a brief review of the literature. *Front. Cardiovasc. Med.* 6:92. doi: 10.3389/fcvm.2019.00092
- Berisha, F., Gotz, K. R., Wegener, J. W., Brandenburg, S., Subramanian, H., Molina, C. E., et al. (2021). cAMP imaging at ryanodine receptors reveals beta2-adrenoceptor driven arrhythmias. *Circ. Res.* 129, 81–94. doi: 10.1161/CIRCRESAHA.120.318234
- Bers, D. M. (2002). Cardiac excitation-contraction coupling. *Nature* 415, 198–205.

- Bers, D. M. (2014). Cardiac sarcoplasmic reticulum calcium leak: basis and roles in cardiac dysfunction. *Annu. Rev. Physiol.* 76, 107–127. doi: 10.1146/annurev-physiol-020911-153308
- Bertero, E., and Maack, C. (2018). Calcium signaling and reactive oxygen species in mitochondria. *Circ. Res.* 122, 1460–1478.
- Bezerides, V. J., Caballero, A., Wang, S., Ai, Y., Hyland, R. J., Lu, F., et al. (2019). Gene therapy for catecholaminergic polymorphic ventricular tachycardia by inhibition of Ca(2+)/calmodulin-dependent kinase II. *Circulation* 140, 405–419. doi: 10.1161/CIRCULATIONAHA.118.038514
- Borile, G., Zaglia, T., Lehnart, S. E., and Mongillo, M. (2021). Multiphoton imaging of Ca(2+) instability in acute myocardial slices from a RyR2(R2474S) murine model of catecholaminergic polymorphic ventricular tachycardia. *J. Clin. Med.* 10:2821. doi: 10.3390/jcm10132821
- Bovo, E., Lipsius, S. L., and Zima, A. V. (2012). Reactive oxygen species contribute to the development of arrhythmogenic Ca(2)(+) waves during beta-adrenergic receptor stimulation in rabbit cardiomyocytes. *J. Physiol.* 590, 3291–3304. doi: 10.1113/jphysiol.2012.230748
- Bovo, E., Mazurek, S. R., De Tombe, P. P., and Zima, A. V. (2015). Increased energy demand during adrenergic receptor stimulation contributes to Ca(2+) wave generation. *Biophys. J.* 109, 1583–1591. doi: 10.1016/j.bpj.2015.09.002
- Boyman, L., Greiser, M., and Lederer, W. J. (2021). Calcium influx through the mitochondrial calcium uniporter holocomplex, MCUcx. *J. Mol. Cell Cardiol.* 151, 145–154. doi: 10.1016/j.yjmcc.2020.10.015
- Boyman, L., Karbowski, M., and Lederer, W. J. (2020). Regulation of mitochondrial ATP production: Ca(2+) signaling and quality control. *Trends Mol. Med.* 26, 21–39. doi: 10.1016/j.molmed.2019.10.007
- Brandenburg, S., Pawlowitz, J., Eikenbusch, B., Peper, J., Kohl, T., Mitronova, G. Y., et al. (2019). Junctophilin-2 expression rescues atrial dysfunction through polyadic junctional membrane complex biogenesis. *JCI Insight* 4:e127116. doi: 10.1172/jci.insight.127116
- Brandes, R., and Bers, D. M. (2002). Simultaneous measurements of mitochondrial NADH and Ca(2+) during increased work in intact rat heart trabeculae. *Biophys. J.* 83, 587–604. doi: 10.1016/S0006-3495(02)75194-1
- Cheng, H., and Lederer, W. J. (2008). Calcium sparks. *Physiol. Rev.* 88, 1491–1545.
- Cooper, L. L., Li, W., Lu, Y., Centracchio, J., Terentyeva, R., Koren, G., et al. (2013). Redox modification of ryanodine receptors by mitochondria-derived reactive oxygen species contributes to aberrant Ca2+ handling in ageing rabbit hearts. *J. Physiol.* 591, 5895–5911. doi: 10.1113/jphysiol.2013.260521
- Cucoranu, I., Clempus, R., Dikalova, A., Phelan, P. J., Ariyan, S., Dikalov, S., et al. (2005). NAD(P)H oxidase 4 mediates transforming growth factor-beta1-induced differentiation of cardiac fibroblasts into myofibroblasts. *Circ. Res.* 97, 900–907. doi: 10.1161/01.RES.0000187457.24338.3D
- Danielsen, T. K., Manotheepan, R., Sadredini, M., Leren, I. S., Edwards, A. G., Vincent, K. P., et al. (2018). Arrhythmia initiation in catecholaminergic polymorphic ventricular tachycardia type 1 depends on both heart rate and sympathetic stimulation. *PLoS One* 13:e0207100. doi: 10.1371/journal.pone.0207100
- Doenst, T., Nguyen, T. D., and Abel, E. D. (2013). Cardiac metabolism in heart failure: implications beyond ATP production. *Circ. Res.* 113, 709–724. doi: 10.1161/CIRCRESAHA.113.300376
- Dooley, C. T., Dore, T. M., Hanson, G. T., Jackson, W. C., Remington, S. J., and Tsien, R. Y. (2004). Imaging dynamic redox changes in mammalian cells with green fluorescent protein indicators. *J. Biol. Chem.* 279, 22284–22293. doi: 10.1074/jbc.M312847200
- Dridi, H., Kushnir, A., Zalk, R., Yuan, Q., Melville, Z., and Marks, A. R. (2020). Intracellular calcium leak in heart failure and atrial fibrillation: a unifying mechanism and therapeutic target. *Nat. Rev. Cardiol.* 17, 732–747. doi: 10.1038/s41569-020-0394-8
- Eisner, D. A., Caldwell, J. L., Trafford, A. W., and Hutchings, D. C. (2020). The control of diastolic calcium in the heart: basic mechanisms and functional implications. *Circ. Res.* 126, 395–412. doi: 10.1161/CIRCRESAHA.119.315891
- Fernandez-Velasco, M., Rueda, A., Rizzi, N., Benitah, J. P., Colombi, B., Napolitano, C., et al. (2009). Increased Ca2+ sensitivity of the ryanodine receptor mutant RyR2R4496C underlies catecholaminergic polymorphic ventricular tachycardia. *Circ. Res.* 104, 201–209. 212p following 209, doi: 10.1161/CIRCRESAHA.108.177493
- Gibbs, C. L., Loiselle, D. S., and Wendt, I. R. (1988). Activation heat in rabbit cardiac muscle. *J. Physiol.* 395, 115–130. doi: 10.1113/jphysiol.1988.sp016911
- Gudbjarnason, S., Hayden, R. O., Wendt, V. E., Stock, T. B., and Bing, R. J. (1962). Oxidation reduction in heart muscle. Theoretical and clinical considerations. *Circulation* 26, 937–945. doi: 10.1161/01.cir.26.5.937
- Guo, Z., Xia, Z., Jiang, J., and McNeill, J. H. (2007). Downregulation of NADPH oxidase, antioxidant enzymes, and inflammatory markers in the heart of streptozotocin-induced diabetic rats by N-acetyl-L-cysteine. *Am. J. Physiol. Heart Circ. Physiol.* 292, H1728–H1736. doi: 10.1152/ajpheart.01328.2005
- Gutschner, M., Pauleau, A. L., Marty, L., Brach, T., Wabnitz, G. H., Samstag, Y., et al. (2008). Real-time imaging of the intracellular glutathione redox potential. *Nat. Methods* 5, 553–559.
- Hamilton, S., Terentyeva, R., Martin, B., Perger, F., Li, J., Stepanov, A., et al. (2020). Increased RyR2 activity is exacerbated by calcium leak-induced mitochondrial ROS. *Basic Res. Cardiol.* 115:38. doi: 10.1007/s00395-020-0797-z
- Hartmann, N., Pabel, S., Herting, J., Schatter, F., Renner, A., Gummert, J., et al. (2017). Antiarrhythmic effects of dantrolene in human diseased cardiomyocytes. *Heart Rhythm* 14, 412–419. doi: 10.1016/j.hrthm.2016.09.014
- Heinzel, F. R., Luo, Y., Dodoni, G., Boengler, K., Petrat, F., Di Lisa, F., et al. (2006). Formation of reactive oxygen species at increased contraction frequency in rat cardiomyocytes. *Cardiovasc. Res.* 71, 374–382. doi: 10.1016/j.cardiores.2006.05.014
- Heymes, C., Bendall, J. K., Ratajczak, P., Cave, A. C., Samuel, J. L., Hasenfuss, G., et al. (2003). Increased myocardial NADPH oxidase activity in human heart failure. *J. Am. Coll. Cardiol.* 41, 2164–2171. doi: 10.1016/s0735-1097(03)00471-6
- Hori, M., and Nishida, K. (2009). Oxidative stress and left ventricular remodeling after myocardial infarction. *Cardiovasc. Res.* 81, 457–464. doi: 10.1093/cvr/cvn335
- Jiang, D., Xiao, B., Zhang, L., and Chen, S. R. (2002). Enhanced basal activity of a cardiac Ca2+ release channel (ryanodine receptor) mutant associated with ventricular tachycardia and sudden death. *Circ. Res.* 91, 218–225. doi: 10.1161/01.res.0000028455.36940.5e
- Jo, H., Noma, A., and Matsuoka, S. (2006). Calcium-mediated coupling between mitochondrial substrate dehydrogenation and cardiac workload in single guinea-pig ventricular myocytes. *J. Mol. Cell Cardiol.* 40, 394–404. doi: 10.1016/j.yjmcc.2005.12.012
- Kohlhaas, M., Nickel, A. G., and Maack, C. (2017). Mitochondrial energetics and calcium coupling in the heart. *J. Physiol.* 595, 3753–3763. doi: 10.1113/JP273609
- Kontula, K., Laitinen, P. J., Lehtonen, A., Toivonen, L., Viitasalo, M., and Swan, H. (2005). Catecholaminergic polymorphic ventricular tachycardia: recent mechanistic insights. *Cardiovasc. Res.* 67, 379–387. doi: 10.1016/j.cardiores.2005.04.027
- Kreitmeier, K. G., Tarnowski, D., Nanadikar, M. S., Baier, M. J., Wagner, S., Katschinski, D. M., et al. (2021). CaMKIIdelta Met281/282 oxidation is not required for recovery of calcium transients during acidosis. *Am. J. Physiol. Heart Circ. Physiol.* 320, H1199–H1212. doi: 10.1152/ajpheart.00040.2020
- Leenhardt, A., Denjoy, I., and Guicheney, P. (2012). Catecholaminergic polymorphic ventricular tachycardia. *Circ. Arrhythm. Electrophysiol.* 5, 1044–1052.
- Lehnart, S. E., Mongillo, M., Bellinger, A., Lindegger, N., Chen, B. X., Hsueh, W., et al. (2008). Leaky Ca2+ release channel/ryanodine receptor 2 causes seizures and sudden cardiac death in mice. *J. Clin. Invest.* 118, 2230–2245. doi: 10.1172/JCI35346
- Lehnart, S. E., Wehrens, X. H., Laitinen, P. J., Reiken, S. R., Deng, S. X., Cheng, Z., et al. (2004). Sudden death in familial polymorphic ventricular tachycardia associated with calcium release channel (ryanodine receptor) leak. *Circulation* 109, 3208–3214. doi: 10.1161/01.CIR.0000132472.98675.EC
- Lieve, K. V. V., Verhagen, J. M. A., Wei, J., Bos, J. M., Van Der Werf, C., Roses, I. N. F., et al. (2019). Linking the heart and the brain: neurodevelopmental disorders in patients with catecholaminergic polymorphic ventricular tachycardia. *Heart Rhythm* 16, 220–228. doi: 10.1016/j.hrthm.2018.08.025
- Liu, N., Colombi, B., Memmi, M., Zissimopoulos, S., Rizzi, N., Negri, S., et al. (2006). Arrhythmogenesis in catecholaminergic polymorphic ventricular tachycardia: insights from a RyR2 R4496C knock-in mouse model. *Circ. Res.* 99, 292–298. doi: 10.1161/01.RES.0000235869.50747.e1
- Liu, N., Rizzi, N., Boveri, L., and Priori, S. G. (2009). Ryanodine receptor and calsequestrin in arrhythmogenesis: what we have learnt from genetic diseases

- and transgenic mice. *J. Mol. Cell Cardiol.* 46, 149–159. doi: 10.1016/j.yjmcc.2008.10.012
- Lu, S., Liao, Z., Lu, X., Katschinski, D. M., Mercola, M., Chen, J., et al. (2020). Hyperglycemia acutely increases cytosolic reactive oxygen species via O-linked GlcNAcylation and CaMKII activation in mouse ventricular myocytes. *Circ. Res.* 126, e80–e96. doi: 10.1161/CIRCRESAHA.119.316288
- Mallilankaraman, K., Doonan, P., Cardenas, C., Chandramoorthy, H. C., Muller, M., Miller, R., et al. (2012). MICU1 is an essential gatekeeper for MCU-mediated mitochondrial Ca(2+) uptake that regulates cell survival. *Cell* 151, 630–644. doi: 10.1016/j.cell.2012.10.011
- Marjamaa, A., Laitinen-Forsblom, P., Wronska, A., Toivonen, L., Kontula, K., and Swan, H. (2011). Ryanodine receptor (RyR2) mutations in sudden cardiac death: studies in extended pedigrees and phenotypic characterization in vitro. *Int. J. Cardiol.* 147, 246–252. doi: 10.1016/j.ijcard.2009.08.041
- Meyer, M., Kewelow, B., Guth, K., Holmes, J. W., Pieske, B., Lehnart, S. E., et al. (1998). Frequency-dependence of myocardial energetics in failing human myocardium as quantified by a new method for the measurement of oxygen consumption in muscle strip preparations. *J. Mol. Cell Cardiol.* 30, 1459–1470. doi: 10.1006/jmcc.1998.0706
- Munzel, T., Camici, G. G., Maack, C., Bonetti, N. R., Fuster, V., and Kovacic, J. C. (2017). Impact of oxidative stress on the heart and vasculature: part 2 of a 3-part series. *J. Am. Coll. Cardiol.* 70, 212–229. doi: 10.1016/j.jacc.2017.05.035
- Murphy, M. P. (2009). How mitochondria produce reactive oxygen species. *Biochem. J.* 417, 1–13.
- Nickel, A. G., Von Hardenberg, A., Hohl, M., Löffler, J. R., Kohlhaas, M., Becker, J., et al. (2015). Reversal of mitochondrial transhydrogenase causes oxidative stress in heart failure. *Cell Metab.* 22, 472–484. doi: 10.1016/j.cmet.2015.07.008
- Peper, J., Kownatzki-Danger, D., Weninger, G., Seibert, F., Pronto, J. R. D., Sutanto, H., et al. (2021). Caveolin3 stabilizes McT1-mediated lactate/proton transport in cardiomyocytes. *Circ. Res.* 128, e102–e120. doi: 10.1161/CIRCRESAHA.119.316547
- Priori, S. G., and Napolitano, C. (2005). Intracellular calcium handling dysfunction and arrhythmogenesis: a new challenge for the electrophysiologist. *Circ. Res.* 97, 1077–1079. doi: 10.1161/01.RES.0000194556.41865.e2
- Rossini, M., and Filadi, R. (2020). Sarcoplasmic reticulum-mitochondria kissing in cardiomyocytes: Ca(2+), ATP, and undisclosed secrets. *Front. Cell Dev. Biol.* 8:532. doi: 10.3389/fcell.2020.00532
- Sadredini, M., Haugsten Hansen, M., Frisk, M., Louch, W. E., Lehnart, S. E., Sjaastad, I., et al. (2021). CaMKII inhibition has dual effects on spontaneous Ca(2+) release and Ca(2+) alternans in ventricular cardiomyocytes from mice with a gain-of-function RyR2 mutation. *Am. J. Physiol. Heart Circ. Physiol.* 321, H446–H460. doi: 10.1152/ajpheart.00011.2021
- Santos, C. X., Anilkumar, N., Zhang, M., Brewer, A. C., and Shah, A. M. (2011). Redox signaling in cardiac myocytes. *Free Radic. Biol. Med.* 50, 777–793.
- Santulli, G., and Marks, A. R. (2015). Essential roles of intracellular calcium release channels in muscle, brain, metabolism, and aging. *Curr. Mol. Pharmacol.* 8, 206–222. doi: 10.2174/1874467208666150507105105
- Santulli, G., Monaco, G., Parra, V., and Morciano, G. (2021). Editorial: mitochondrial remodeling and dynamic inter-organellar contacts in cardiovascular physiopathology. *Front. Cell Dev. Biol.* 9:679725. doi: 10.3389/fcell.2021.679725
- Santulli, G., Pagano, G., Sardu, C., Xie, W., Reiken, S., D'ascia, S. L., et al. (2015). Calcium release channel RyR2 regulates insulin release and glucose homeostasis. *J. Clin. Invest.* 125, 4316.
- Satoh, H., Blatter, L. A., and Bers, D. M. (1997). Effects of [Ca<sup>2+</sup>]<sub>i</sub>, SR Ca<sup>2+</sup> load, and rest on Ca<sup>2+</sup> spark frequency in ventricular myocytes. *Am. J. Physiol.* 272, H657–H668. doi: 10.1152/ajpheart.1997.272.2.H657
- Shan, J., Xie, W., Betzenhauser, M., Reiken, S., Chen, B. X., Wronska, A., et al. (2012). Calcium leak through ryanodine receptors leads to atrial fibrillation in 3 mouse models of catecholaminergic polymorphic ventricular tachycardia. *Circ. Res.* 111, 708–717. doi: 10.1161/CIRCRESAHA.112.273342
- Suga, H. (1990). Ventricular energetics. *Physiol. Rev.* 70, 247–277.
- Swain, L., Kesemeyer, A., Meyer-Roxlau, S., Vettel, C., Ziesenis, A., Guntsch, A., et al. (2016). Redox imaging using cardiac myocyte-specific transgenic biosensor mice. *Circ. Res.* 119, 1004–1016. doi: 10.1161/CIRCRESAHA.116.309551
- Takimoto, E., Champion, H. C., Li, M., Ren, S., Rodriguez, E. R., Tavazzi, B., et al. (2005). Oxidant stress from nitric oxide synthase-3 uncoupling stimulates cardiac pathologic remodeling from chronic pressure load. *J. Clin. Invest.* 115, 1221–1231. doi: 10.1172/JCI21968
- Tester, D. J., Dura, M., Carturan, E., Reiken, S., Wronska, A., Marks, A. R., et al. (2007). A mechanism for sudden infant death syndrome (SIDS): stress-induced leak via ryanodine receptors. *Heart Rhythm* 4, 733–739. doi: 10.1016/j.hrthm.2007.02.026
- Uchinoumi, H., Yano, M., Suetomi, T., Ono, M., Xu, X., Tateishi, H., et al. (2010). Catecholaminergic polymorphic ventricular tachycardia is caused by mutation-linked defective conformational regulation of the ryanodine receptor. *Circ. Res.* 106, 1413–1424. doi: 10.1161/CIRCRESAHA.109.209312
- von Harsdorf, R., Li, P. F., and Dietz, R. (1999). Signaling pathways in reactive oxygen species-induced cardiomyocyte apoptosis. *Circulation* 99, 2934–2941. doi: 10.1161/01.cir.99.22.2934
- Wagner, E., Brandenburg, S., Kohl, T., and Lehnart, S. E. (2014). Analysis of tubular membrane networks in cardiac myocytes from atria and ventricles. *J. Vis. Exp.* 92:e51823. doi: 10.3791/51823
- Wagner, E., Lauterbach, M. A., Kohl, T., Westphal, V., Williams, G. S., Steinbrecher, J. H., et al. (2012). Stimulated emission depletion live-cell super-resolution imaging shows proliferative remodeling of T-tubule membrane structures after myocardial infarction. *Circ. Res.* 111, 402–414. doi: 10.1161/CIRCRESAHA.112.274530
- Wehrens, X. H., Lehnart, S. E., Huang, F., Vest, J. A., Reiken, S. R., Mohler, P. J., et al. (2003). FKBP12.6 deficiency and defective calcium release channel (ryanodine receptor) function linked to exercise-induced sudden cardiac death. *Cell* 113, 829–840. doi: 10.1016/s0092-8674(03)00434-3
- Wescott, A. P., Kao, J. P. Y., Lederer, W. J., and Boyman, L. (2019). Voltage-energized calcium-sensitive ATP production by mitochondria. *Nat. Metab.* 1, 975–984.
- Wlekinski, M. J., Kannankeril, P. J., and Knollmann, B. C. (2020). Molecular and tissue mechanisms of catecholaminergic polymorphic ventricular tachycardia. *J. Physiol.* 598, 2817–2834. doi: 10.1113/JP276757
- Xie, W., Santulli, G., Reiken, S. R., Yuan, Q., Osborne, B. W., Chen, B. X., et al. (2015). Mitochondrial oxidative stress promotes atrial fibrillation. *Sci. Rep.* 5:11427. doi: 10.1038/srep11427
- Yano, M., Okuda, S., Oda, T., Tokuhisa, T., Tateishi, H., Mochizuki, M., et al. (2005). Correction of defective interdomain interaction within ryanodine receptor by antioxidant is a new therapeutic strategy against heart failure. *Circulation* 112, 3633–3643. doi: 10.1161/CIRCULATIONAHA.105.555623
- Yano, M., Yamamoto, T., Kobayashi, S., and Matsuzaki, M. (2009). Role of ryanodine receptor as a Ca(2+)(+) regulatory center in normal and failing hearts. *J. Cardiol.* 53, 1–7. doi: 10.1016/j.jjcc.2008.10.008
- Zhou, B., and Tian, R. (2018). Mitochondrial dysfunction in pathophysiology of heart failure. *J. Clin. Invest.* 128, 3716–3726. doi: 10.1172/JCI120849

**Conflict of Interest:** The authors declare that the research was conducted in the absence of any commercial or financial relationships that could be construed as a potential conflict of interest.

**Publisher's Note:** All claims expressed in this article are solely those of the authors and do not necessarily represent those of their affiliated organizations, or those of the publisher, the editors and the reviewers. Any product that may be evaluated in this article, or claim that may be made by its manufacturer, is not guaranteed or endorsed by the publisher.

Copyright © 2021 Wegener, Wagdi, Wagner, Katschinski, Hasenfuss, Bruegmann and Lehnart. This is an open-access article distributed under the terms of the Creative Commons Attribution License (CC BY). The use, distribution or reproduction in other forums is permitted, provided the original author(s) and the copyright owner(s) are credited and that the original publication in this journal is cited, in accordance with accepted academic practice. No use, distribution or reproduction is permitted which does not comply with these terms.